2006-06-26

Compact and low loss silicon-on-insulator rib waveguide 90° bend

Yusheng Qian
Brigham Young University - Provo, qianyusheng@gmail.com

Seunghyun Kim
Brigham Young University - Provo, shkim@ee.byu.edu

Jiguo Song
Brigham Young University - Provo

Gregory P. Nordin
Brigham Young University - Provo, nordin@byu.edu

Jianhua Jiang
University of Alabama - Huntsville

Follow this and additional works at: https://scholarsarchive.byu.edu/facpub

Part of the Electrical and Computer Engineering Commons

Original Publication Citation

Yusheng Qian, Seunghyun Kim, Jiquo Song, Gregory P. Nordin, and Jianhua Jiang, "Compact and low loss silicon-on-insulator ridge waveguide 9° bend," Optics Express 14, pp. 62-628 (26).

BYU ScholarsArchive Citation

Qian, Yusheng; Kim, Seunghyun; Song, Jiguo; Nordin, Gregory P.; and Jiang, Jianhua, "Compact and low loss silicon-on-insulator rib waveguide 90° bend" (2006). *Faculty Publications*. 1420.
https://scholarsarchive.byu.edu/facpub/1420

Compact and low loss silicon-on-insulator rib waveguide 90° bend

Yusheng Qian, Seunghyun Kim, Jiguo Song, and Gregory P. Nordin

Electrical and Computer Engineering, Brigham Young University,Provo, UT 84602 USA
shkim@ee.byu.edu

Jianhua Jiang

Nano and Micro Devices Center, University of Alabama in Huntsville, Huntsville AL 35899 USA

Abstract: A compact and low loss silicon-on-insulator rib waveguide 90° bend is designed and demonstrated. An interface realized by a trench filled with SU8 at the corner of a waveguide bend effectively reflects incoming light through total internal reflection (TIR). In order to accurately position the SU8-filled trench relative to the waveguide and reduce sidewall roughness of the interface, electron beam lithography (EBL) is employed while inductively coupled plasma reactive ion etching (ICP RIE) is used to achieve a vertical sidewall. The measured loss for TE polarization is 0.32 dB ± 0.02 dB/bend at a wavelength of 1.55 μm.

References and Links

1. Y. Z. Tang, W. H. Wang, T. Li, and Y. L. Wang, "Integrated waveguide turning mirror in silicon-on-insulator," IEEE Photon. Technol. Lett. **14**, 68-70 (2002).
2. S. Ladenois, D. Pascal, L. Vivien, E. Cassan, S. Laval, R. Orobtchouk, M. Heitzmann, N. Bouzaida, and L. Mollard, "Low-loss submicrometer silicon-on-insulator rib waveguides and corner mirrors," Opt. Lett. **28**, 1150-1152 (2003).
3. J. Liu, J. Yu, S. Chen, and Z. Li, "Integrated folding 4 X 4 optical matrix switch with total internal reflection mirrors on SOI by anisotropic chemical etching," IEEE Photon. Technol. Lett. **17**, 1187-1189 (2005).
4. R. U. Ahmad, F. Pizzuto, G. S. Camarda, R. L. Espinola, H. Rao, and R. M. Osgood, Jr., "Ultracompact corner-mirrors and T-branches in silicon-on-insulator," IEEE Photon. Technol. Lett. **14**, 65-67 (2002).
5. Y. A. Vlasov and S. J. McNab, "Losses in single-mode silicon-on-insulator strip waveguides and bens," Opt. Express **12**, 1622-1631 (2004).
6. A. Vorckel, M. Moster, W. Henschel, P. H. Bolivar, and H. Kurz, "Asymmetrically coupled silicon-on-insulator microring resonators for compact add-drop multiplexers," IEEE Photon. Technol. Lett. **15**, 921-923 (2003).
7. I. Kiyat, A. Aydinli, and N. Dagli, "High-Q silicon-on-insulator optical rib waveguide racetrack resonators," Opt. Express **13**, 1900-1905 (2005).
8. P. Dumon, W. Bogaerts, V. Wiaux, J. Wouters, S Beckx, J. V. Campenhout, D. Taillaert, B. Luyssaert, P. Bienstman, D. V. Thourhout, and R. Baets, "Low-loss SOI photonic wires and ring resonators fabricated with deep UV lithography," IEEE Photon. Technol. Lett. **16**, 1328-1330 (2004).
9. T. Tsuchizawa, K. Yamada, H. Fukuda, T. Watanabe, J. Takahashi, M. Takahashi, T. Shoji, E. Tamechika, S. Itabashi, and H. Morita, "Microphotonics devices based on silicon microfabrication technology," IEEE J. Sel. Topics Quantum Electron. **11**, 232-240 (2005).
10. B. Jalali, S. Yegnanarayanan, T. Yoon, T. Yoshimoto, I. Rendina, and F. Coppinger, "Advances in silicon-on-insulator optoelectronics," IEEE J. Sel. Top. Quantum Electron. **4**, 938-947 (1998).

11. P. Dainesi, A. Kung, M. Chabloz, A. Lagos, Ph. Fluckiger, A. Ionescu, P. Fazan, M. Declerq, Ph. Renaud, and Ph. Robert, "CMOS compatible fully integrated mach-zehnder interferometer in SOI technology," IEEE Photon. Technol. Lett. **12**, 660-662 (2000).
12. C. Angulo Barrios, V. R. Almeida, R. Panepucci, and M. Lipson, "Electrooptic modulation of silicon-on-insulator submicrometer-size waveguide devices," J. Lightwave Technol. **21**, 2332-2338 (2003).
13. S. F. Preble, Q. Xu, B. S. Schmidt, and M. Lipson, "Ultrafast all-optical modulation on a silicon chip," Opt. Lett. **30**, 2891-2893 (2005).
14. R. Jones, A. Liu, H. Rong, and M. Paniccia, "Lossless optical modulation in a silicon waveguide using stimulated Raman scattering," Opt. Express **13**, 1716-1723 (2005).
15. O. Boyraz and B. Jalali, "Demonstration of a silicon Raman laser," Opt. Express **12**, 5269-5273 (2004).
16. H. Rong, A. Liu, R. Jones, O. Cohen, D. Hak, R. Nicolaescu, A. Fang, and M. Paniccia, "An all-silicon Raman laser," Nature **433**, 292-294 (2005).
17. A. Taflove, *Computational Electrodynamics: The Finite-Difference Time-Domain Method* (Artech House, Boston, Mass.,1995).
18. J. P. Berenger, "A perfectly matched layer for the absorption of electromagnetic waves," J. Comput. Phys. **114**, 185-200 (1994).
19. J. Cai, G. P. Nordin, S. Kim, and J. Jiang, "Three-dimensional analysis of a hybrid photonic crystal-conventional waveguide 90° bend," Appl. Opt. **43**, 4244-4249 (2004).
20. M. J. Madou, "Lithography," in *Fundamentals of Microfabrication: The Science of Miniaturization, 2nd ed.* (CRC Press, Fla., 2002) pp. 28-29.

1. Introduction

Silicon-on-insulator (SOI) waveguides have received much attention as a platform for planar lightwave circuits (PLCs) in recent years because of their compatibility with complementary metal oxide semiconductor (CMOS) technologies and the possibility of combining PLCs and microelectronics on a single chip [1-16]. Passive [1-9] and active [10-14] PLCs on SOI have been designed and demonstrated. Recently, the appearance of Raman-based lasers in SOI waveguides has increased the possibility of realizing fully integrated lasers, active and passive PLCs, and microelectronics [15,16].

Light in the silicon layer of SOI is naturally confined in the vertical direction because of the high index contrast between the bottom oxide layer, Si layer, and air. By removing part (rib) or all (channel) of the silicon layer around the waveguide core in the horizontal plane, SOI waveguides are realized. To maximize the level of integration of PLCs on a single SOI chip, compact and low loss SOI waveguide bends are required. The radius of curvature of a conventional waveguide bend is determined by the index contrast of the waveguide in the horizontal plane. For channel waveguides in which the index contrast in the horizontal plane is large, low loss waveguide bends with < 2 µm radius of curvature have been reported [4,5]. However, in the case of rib waveguides, the refractive index difference in the horizontal plane is relatively small, and thus the radius of curvature for a conventional waveguide bend is much larger.

Single air interface bends for SOI rib waveguides have been reported [1-3] as a method of achieving compact bends in which light propagating in an input waveguide is reflected by an interface through total internal reflection (TIR) into an output waveguide. Tang *et al.* [1] reported an air trench turning mirror for a rib waveguide with a loss of less than 0.5 dB/bend formed using potassium hydroxide (KOH) wet chemical etching. However, direct measurement data is not presented. Lardenois *et al.* [2] used reactive ion etching (RIE) to realize an air trench for a rib waveguide bend. The measured loss is 1 dB/bend which is comparable to other results found in the literature for KOH etched bends [3].

In this paper, we report a compact and low loss SOI rib waveguide 90° bend with a SU8-filled trench. The measured loss is 0.32 ± 0.02dB/bend. We employ electron beam lithography (EBL) to accurately position the trench interface relative to the input and output waveguides and to reduce the roughness of the interface. Inductively coupled plasma reactive ion etching (ICP RIE) is used to achieve an anisotropic trench etch with vertical sidewalls. We first

present the design of the bend structure and discuss the SU8 interface position tolerance. Then we discuss the fabrication process and measurement results.

2. SOI rib waveguide bend design

As shown in Fig. 1(a), our SOI rib waveguide has a silicon layer thickness of 0.75 μm, etch depth of 0.1 μm, and rib width of 1.6 μm. It supports only the fundamental TE polarization (electric field in the plane) mode at a wavelength of 1.55 μm. Therefore, bend design and measurement are performed only for TE polarization. Refractive indices of silicon and silicon dioxide used for a SOI rib waveguide design are 3.477 and 1.444, respectively. For the upper clad, we choose either air (n = 1.0) or SU8 (n = 1.57) depending on whether SU8 is used in the trenches or not. Fig. 1(b) shows the fundamental TE polarization mode calculated by FIMMWAVE (Photon Design) with a SU8 upper clad.
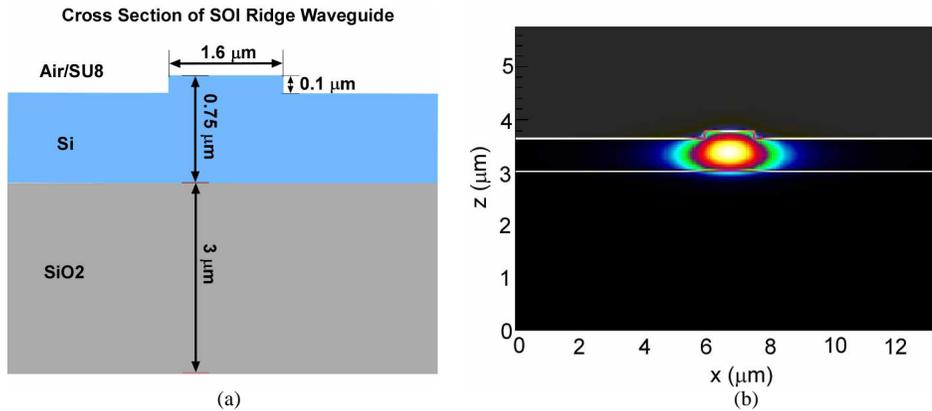

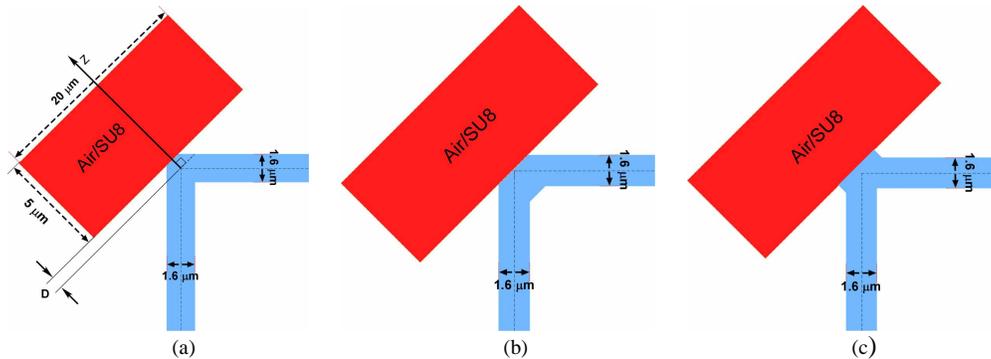Fig. 1. (a) Cross section and (b) fundamental TE mode of single mode SOI rib waveguide.

Fig. 2. SOI rib waveguide bend geometries: (a) Right angle bend (Case 1), (b) right angle bend with additional core at the inner side of bend corner (Case 2) [1], and (c) right angle bend with additional core at the outer side of bend corner (Case 3) [2]. 'D' in Fig. 2(a) is defined as the distance from the intersection of the center lines of the input and output waveguides to the interface between air/SU8-filled trench and SOI rib waveguide region.

We use the two dimensional (2-D) finite difference time domain (FDTD) method [17] with Berenger perfectly matched layer (PML) boundary conditions [18] to numerically calculate 2-D bend efficiencies. The SOI rib waveguide structure is approximated as a 2-D structure for these calculations. For an air upper cladding, the 2-D effective core and clad refractive indices are 3.370 and 3.340, while for a SU8 upper cladding they are 3.371 and 3.343, respectively.

A number of different bend geometries have been reported in the literatures, which are shown in Fig. 2. We use 2-D FDTD simulation to determine which structure offers the most promise to achieve high bend efficiency. In each case we evaluate both air and SU8 for the upper clad and trench fill material. Because out-of-plane losses at the interface of a bend corner are not accounted for in 2-D FDTD simulation, we employ the perfect mirror model discussed in Ref. 19 to estimate the 3-D performance of each bend geometry. Since the perfect mirror model shows good agreement with the 3-D FDTD method [19], it provides a simple way to calculate 3-D structure performance without the computational burden of doing actual 3-D FDTD calculations.

With the perfect mirror model, the bend efficiency, η, is calculated as

$$\eta = \Gamma_{FF} \, \eta_{2D} \tag{1}$$

where η_{2D} is the bend efficiency calculated by 2-D FDTD with a mode overlap integral (MOI) method (i.e., the ratio of the power in the guided mode in the output waveguide to the power in the incident guided mode) and Γ_{FF} is the filling factor calculated as the ratio of the optical power confined in the silicon layer to the optical power of the fundamental mode:

$$\Gamma_{FF} = \frac{\int^R P(s)ds}{\int^\infty P(s)ds} \tag{2}$$

The filling factors are calculated with FIMMWAVE.

Table 1 shows calculation results for TE polarization for all 6 cases at $\lambda = 1.55$ μm. The trench position is fixed to be D = - 70 nm for all cases (D is defined in Fig. 2(a)) to account for the Goos-Hanchen shift. Note that there is very little difference in the bend efficiency between the different cases. Since the Si refractive index is so much higher than either air or SU8, the filling factor is nearly identical. The 2-D FDTD results show that given a particular fill material (air or SU8), the details of the waveguide corner structure make very little difference, although the SU8 fill is slightly better than air. The main advantage of the SU8 is that is protects the TIR interface from contaminants such as particulates that can spoil the TIR effect.

Table 1. Calculated bend efficiencies of three different structures filled with either air or SU8.

	η_{2D}	Γ_{FF}	η
Case 1 with air	0.988	0.986	0.974
Case 1 with SU8	0.995	0.985	0.980
Case 2 with air	0.987	0.986	0.973
Case 2 with SU8	0.995	0.985	0.980
Case 3 with air	0.993	0.986	0.979
Case 3 with SU8	0.995	0.985	0.980

Since the simulation results are all so close, we selected the simplest structure (Case 1) for fabrication. Figure 3(a) shows the magnitude squared time averaged magnetic field for this structure at a wavelength of 1.55 μm. The bend efficiency as a function of D is shown in Fig. 3(b). The maximum bend efficiency is obtained at D = - 70 nm because of the Goos-Hanchen shift.
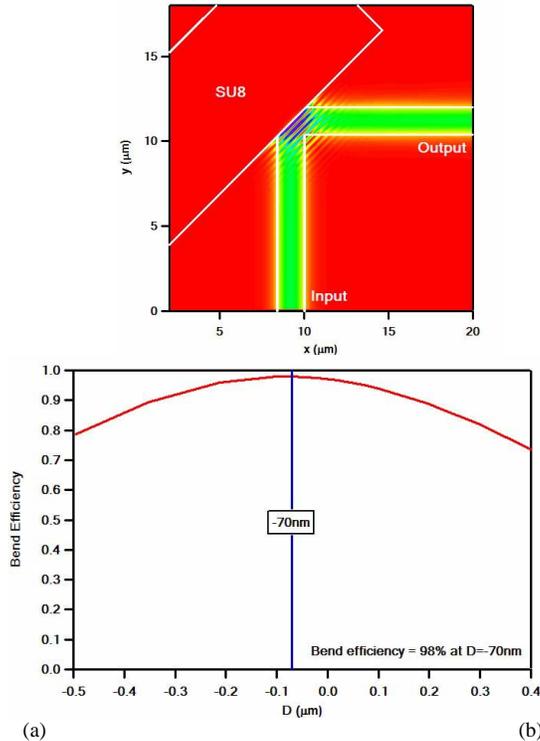
Fig. 3. (a) Magnitude squared time averaged magnetic field and (b) bend efficiency as a function of 'D' of compact and low loss SOI waveguide bend design at $\lambda = 1.55$ µm.

Figure 3(b) shows not only the best SU8 interface position to achieve the maximum bend efficiency but also the tolerance with respect to interface position. If the interface is misplaced more than ± 0.25 µm from the ideal position, the bend efficiency decreases to below 90 %. The positioning is therefore very important to achieve high efficiency bends for SOI rib waveguides.

3. Fabrication

We employ electron beam lithography (EBL) for fabricating low loss SOI rib waveguide bends. A LEO 1550 field emission scanning electron microscope (FESEM) with a nanometer pattern generation system (NPGS) (JC Nabity Lithography Systems) is used for EBL. Compared to optical lithography in an available contact mask aligner, EBL shows very high alignment accuracy and smoother sidewalls after patterning.

We first determine the alignment accuracy of EBL with the use of Vernier structures [20]. A typical EBL alignment test result is shown in Fig. 4. Note that the EBL written patterns are well-centered on the matching substrate patterns. Since the difference in periods between the two is 40 nm, the alignment accuracy is somewhere below 40 nm, which is compatible with the required interface positioning tolerance to achieve high bend efficiency.
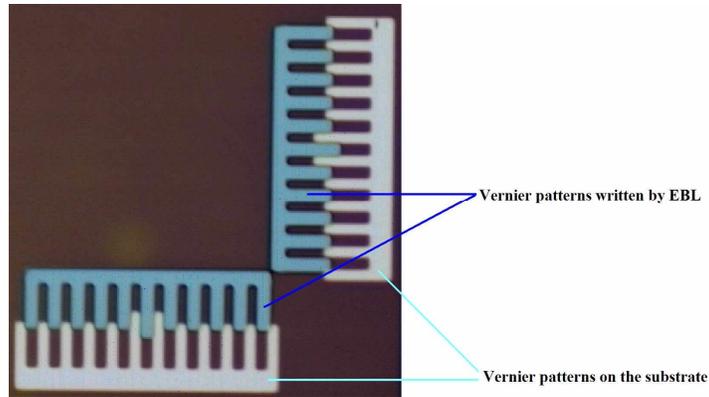
Fig. 4. Vernier patterns to determine alignment accuracy of EBL along X and Y directions.

Figure 5 shows the bend fabrication process flow. We start with a SOITEC SOI wafer with a 0.75 μm Si layer on a 3.0 μm oxide layer. Gold alignment marks for EBL alignment are optically patterned in the same patterning step as the SOI waveguide ribs for accurate alignment of the trenches relative to the waveguides. Cr is used as an adhesion layer for Au on the silicon surface. Optically patterned alignment marks are transferred to the Au and Cr layers by wet chemical etching. Then the SOI waveguide rib is defined by ICP RIE etching 0.1 μm of the silicon layer using a C_4F_8 and SF_6 chemistry. Positive electron beam resist (ZEP 520A) is spun on top of the SOI rib waveguides and Au EBL alignment marks. After exposure, the EBL patterned trenches are then etched with ICP RIE to a depth of 0.75 μm using a C_4F_8 and SF_6 chemistry. Finally, SU8 is spun on top to fill the air trenches and cover the surface.
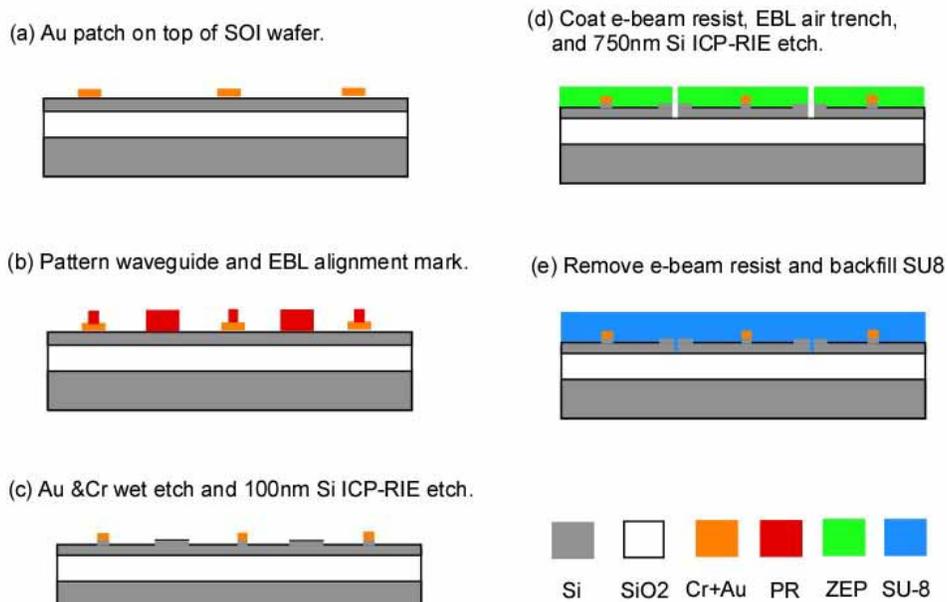

Fig. 5. Fabrication process of compact and high efficiency SOI rib waveguide bend with SU8 filled trench.

To measure the bend efficiency of SOI rib waveguide bends with SU8-filled trenches, we designed SOI rib waveguide bend structures with different numbers of bends (4, 8, 12, 16, and 20 bends) while keeping the waveguide length the same. Figure 6 shows scanning electron microscope (SEM) images of SOI rib waveguide bends after the silicon etch to define the trenches and before SU8 spin coating.

Figure 7 shows details of the interface sidewall roughness. We observe vertical sidewalls with only a small amount of roughness. Note also the roughness along the waveguide ribs, which are patterned with optical contact lithography. Comparing roughness along the waveguide rib and on the interface sidewall, we can see that EBL results in a smoother edge. Since all waveguides have the same length, scattering loss from the rib edge roughness of the waveguides doesn't affect our optical bend efficiency measurements.
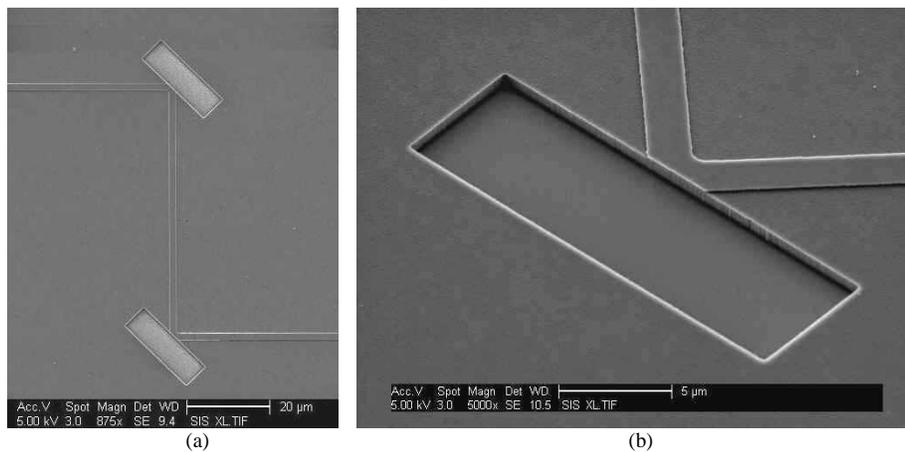

Fig. 6. SEM images of (a) 2 bends and (b) close up of a single bend after trench etch and before SU8 spin coating.
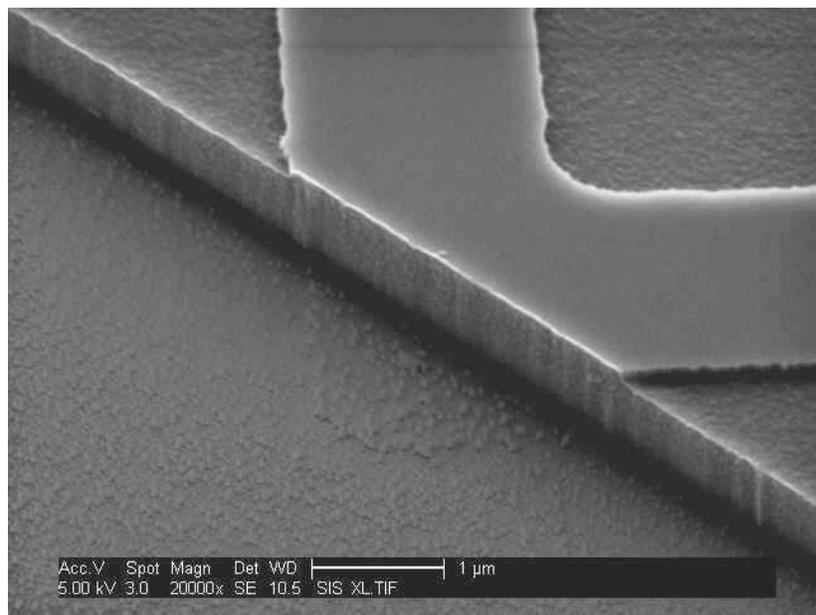

Fig. 7. SEM image of interface of trench and SOI rib waveguide showing roughness of the interface sidewall.

4. Experimental measurement and discussion

To measure optical power loss from a set of SOI rib waveguides with different numbers of bends, TE polarized light from a polarization maintaining (PM) fiber connected to a superluminescent light emitting diode (SLED) with a center wavelength of 1.55 μm is butt coupled to an input waveguide. A single mode fiber is butt coupled to the corresponding output waveguide. A Newport autoalign system is used to align the input fiber, device, and output fiber. The input and output fiber positions are optimized to maximize optical outputs by computer controlled three axis translation stages which have 50 nm movement resolution.

Figure 8 shows the measured optical loss as a function of the number of bends in a waveguide. The measured bend loss is 0.32 ± 0.02 dB/bend (92.9 % bend efficiency) which is the lowest SOI rib waveguide 90° bend loss reported in the literature to the best of our knowledge. Since the maximum achievable calculated bend efficiency is 98.0 %, there is still some room for improvement, which most likely can be achieved by further reducing the interface sidewall roughness.
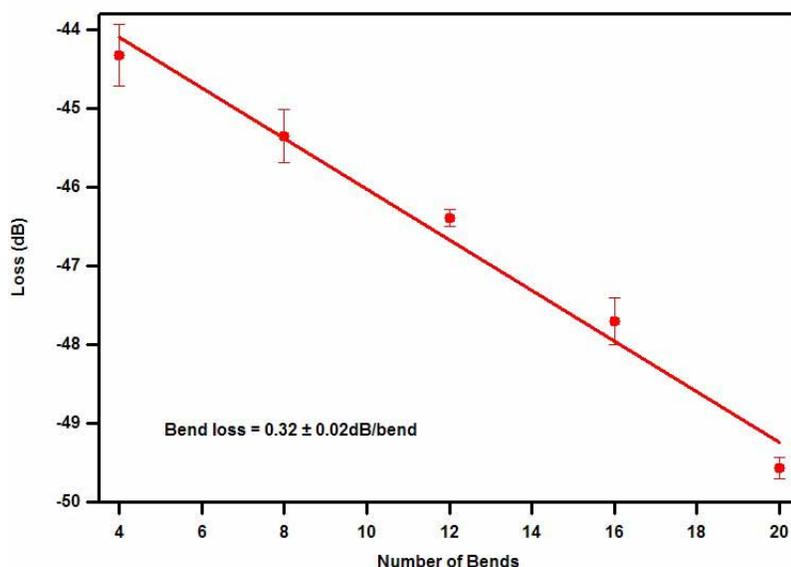

Fig. 8. Measured loss of compact SOI rib waveguide bend with SU8 filled trench as a function of number of bends at $\lambda = 1.55$ μm.

5. Summary

Compact and low loss SOI rib waveguide 90° bends with SU8 filled trenches have been designed and experimentally demonstrated. Three different structures with an air or a SU8-filled trench are numerically simulated and compared to determine the final structure for fabrication. The perfect mirror model is employed to calculate the bend structure performance. EBL and ICP-RIE processes are used to fabricate the designed bends. With EBL, very accurate SU8 interface positioning relative to waveguides is accomplished and the roughness on the interface sidewall is reduced while vertical interface sidewalls are realized by ICP-RIE. Compact SOI rib waveguide bend loss is then experimentally measured. The bend loss is 0.32 ± 0.02 dB/bend (92.9 % bend efficiency) for TE polarization at $\lambda = 1.55$ μm which is the lowest loss of a SOI rib waveguide 90° bend reported in literature to the best of our knowledge.

Acknowledgment